

# Active Fusion and Fission Processes on a Fluid Membrane

Madan Rao<sup>1,2\*</sup> and Sarasij R. C.<sup>1,3†</sup>

<sup>1</sup>Raman Research Institute, C.V. Raman Avenue, Sadashivanagar, Bangalore 560080, India

<sup>2</sup>National Centre for Biological Sciences, UAS-GKVK Campus, Bellary Road, Bangalore 560065, India

<sup>3</sup>Institute of Mathematical Sciences, Taramani, Chennai 600113, India

(October 24, 2018)

We investigate the steady states and dynamical instabilities resulting from “particles” depositing on (fusion) and pinching off (fission) a fluid membrane. These particles could be either small lipid vesicles or isolated proteins. In the stable case, such fusion/fission events suppress long wavelength fluctuations of the membrane. In the unstable case, the membrane shoots out long tubular structures reminiscent of endosomal compartments or folded structures as in internal membranes like the endoplasmic reticulum or Golgi.

PACS numbers: 87.16.-b, 05.40.-a, 82.65.Dp

The plasma membrane and internal membranes of eukaryotic cells such as endosomal compartments, Golgi and endoplasmic reticulum (ER) are subject to random deposition and evaporation of ‘particles’ [1]. These particles could be isolated lipids or membrane proteins but most often are small vesicles carrying cargo. For instance, in the endocytic pathway, small vesicles (diameter  $\approx 50\text{nm}$ ), pinch off from the plasma membrane and fuse with the sorting endosome. The sorting endosome is seen to possess long, thin, tubular protrusions that sporadically break away from it [2]. Likewise the ER  $\longleftrightarrow$  Golgi  $\longleftrightarrow$  Plasma Membrane system [3] witnesses a major trafficking of protein carrying vesicles. The Golgi and the ER are highly ramified membranal structures, often possessing long thin tubular protrusions [1].

The fusion/fission events are ‘active’ processes in that they are triggered by signalling proteins which recruit an elaborate array of proteins as part of the fusion/fission machinery [1,3]. These proteins, such as coat proteins, SNARES and rabs are functionally activated by energy provided by the consumption of ATP/GTP. Though at first sight the phenomenon appears alarmingly complex, we argue below that it gives rise to precise questions of a generic nature that do not require a knowledge of specific biomolecular details, and which may be addressed within the framework of nonequilibrium statistical physics.

In this Letter we ask: Starting with an almost planar fluid membrane, what is its eventual shape when subject to such active fusion/fission events? We will find that the final fate of the membrane is (a) a steady state shape whose long wavelength fluctuations are suppressed by such events or (b) a dynamical instability giving rise to either long tubular structures or folded structures which grow rapidly. This rapid growth would be halted by other processes (not included in our analysis) which might lead to an eventual pinch off from the membrane.

We take a coarse-grained approach in which the equilibrium shapes of a fluid membrane (in the absence of fusion/fission), parametrized by its 3-dimensional conformation  $\mathbf{R}(u_1, u_2)$  as a function of local coordinates  $(u_1, u_2)$ , are governed by the local curvature [4] and the

areal density  $\tilde{\psi}$  of ‘particles’ on it, through the effective free-energy functional

$$F_{el} = \frac{1}{2} \int d^2u \sqrt{g} \left[ \sigma + \kappa_c H^2 + 2c_0 \tilde{\psi} H + \chi \tilde{\psi}^2 \right]. \quad (1)$$

The local mean curvature  $H = 1/2 g_{ab} \hat{\mathbf{N}} \cdot \partial_a \partial_b \mathbf{R}$ , where  $\hat{\mathbf{N}}$  is the local unit (outward) normal and  $g_{ab}$  is the induced metric ( $g \equiv \det g_{ab}$ ). The density field  $\tilde{\psi}$  has the following interpretation — when the particles are tiny lipid vesicles,  $\tilde{\psi} = \tilde{\rho} - \tilde{\rho}_0$  is the excess areal lipid density ( $\tilde{\rho}$  is the local areal lipid density and  $\tilde{\rho}_0$  is its equilibrium value) and  $c_0 = 0$ ; when the particles are isolated membrane proteins or structurally asymmetric transmembrane proteins,  $\tilde{\psi}$  is the areal protein density and the spontaneous curvature modulus  $c_0 \neq 0$ , reflecting the change in the local elastic properties of the membrane due to the embedded protein.

In this paper we will work entirely in the Monge representation where the membrane shape is represented by a height field  $h(x, y)$  and all physical quantities are computed in the horizontal  $\mathbf{x} \equiv (x, y)$  plane. In this representation  $g = 1 + (\nabla h)^2$  and  $H = \nabla^2 h / g^{3/2}$ . The areal densities projected onto the  $\mathbf{x}$  plane are obtained from  $\rho = \tilde{\rho} \sqrt{g}$ . In our notation quantities with and without the tilde will denote intrinsic and projected densities respectively. In this Monge representation, thermal equilibrium height correlations are given by  $\langle |h_q|^2 \rangle \propto T / (\sigma q^2 + \kappa_R q^4)$ , where  $\kappa_R = \kappa_c - (\kappa_c c_0)^2 / \chi$ .

We now start the fusion/fission processes which drive the membrane out of equilibrium, giving rise to a dynamical excess density field  $\psi(\mathbf{x}, t)$  and a dynamical shape  $h(\mathbf{x}, t)$ . For convenience we shall use the *picture* of fusion/fission of small vesicles in the rest of the paper, although our mathematical treatment includes the deposition and ‘evaporation’ of isolated proteins as well. Our subsequent analysis is valid over length scales much larger than the typical size  $\ell$  of the ‘particles’ and time scales much longer than the duration of individual fusion(fission)-events  $\tau$ . Thus we shall ignore the complicated microscopic processes at work during the event. As

in [5], we try to extract the most robust features through general symmetry arguments. To facilitate analysis, we can regard a local region of the membrane as being in one of three states: (i) an undistorted membrane; (ii) a membrane with a ‘bump’; (iii) an undistorted membrane with a proximate vesicle. The balance between (i) and (ii) is governed largely by elastic and equilibrium thermodynamic forces whereas that between (ii) and (iii) is determined mainly by active processes [6] (Fig. 1).

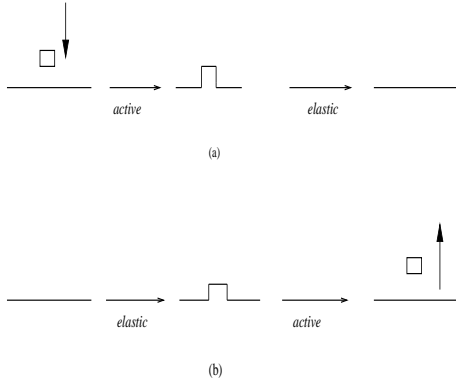


FIG. 1. The ‘active’ and ‘elastic’ stages of (a) fusion and (b) fission.

Define an ‘fusion-event’  $\epsilon_+(\mathbf{x}, t)$  and an ‘fission-event’  $\epsilon_-(\mathbf{x}, t)$  as random numbers taking values 0 or 1, with a nonzero mean  $\langle \epsilon_{\pm} \rangle = e_{\pm}$  and distributed identically and independently at different  $\mathbf{x}$  and  $t$ . Every event gives rise to a change in the local height and density; we would therefore like to calculate the rate of such fusion/fission events (number of events/area/time). We argue as follows: Since the fusion/fission-events happen only on the cytosolic side in the case of internal membranes, and in an in-out asymmetric manner in the case of the plasma membrane, a local observer on the membrane can tell up from down in the Monge description. Thus all dynamical effects should reflect this up/down membrane asymmetry. This implies that the rate of fusion(fission) events,  $r^+(r^-)$ , should be sensitive to the local mean curvature and hence to lowest order can be written as

$$r_n^+ = \lambda_1 + \lambda_2 H + \lambda_3 \tilde{\rho} + \lambda_4 \tilde{\rho} H + \dots \quad (2)$$

$$r_n^- = \mu_1 \tilde{\rho} + \mu_2 \tilde{\rho} H + \dots \quad (3)$$

where the coefficients  $\lambda_1, \mu_1 > 0$  by virtue of the definition of the fusion/fission processes. Note that symmetry arguments say nothing about the values of the other parameters, whose magnitudes and signs are determined by the microphysics of fusion/fission.

To determine the net normal velocity, we multiply the above rates by a typical velocity  $\ell/\tau$  and include a permeative contribution proportional to the force  $f_{el} \equiv \delta F_{el}/\delta \mathbf{R}$ ,

$$v_n = (\ell/\tau) [\epsilon_+(x, t) r_n^+ - \epsilon_-(x, t) r_n^-] - \Gamma f_{el}, \quad (4)$$

where  $\Gamma$  is a mobility. Similarly the changes in the density due to the fusion/fission events are proportional to the ‘particle currents’,

$$j_+ = (A_+/\tau) \epsilon_+(\mathbf{x}, t) r_n^+ \quad (5)$$

$$j_- = (A_-/\tau) \epsilon_-(\mathbf{x}, t) r_n^- \quad (6)$$

where  $A_{\pm}$  are dimensionless, positive constants. It will turn out that we may consistently take  $A_+ = A_-$  (for lipid vesicles,  $A_+ = \ell^2/a$ , the amount of lipid material brought during a typical fusion event,  $a$  being the area per lipid).

In the Monge representation, we decompose the normal velocity along the vertical  $z$  axis,  $v_z = v_n(\hat{\mathbf{N}} \cdot \hat{\mathbf{z}})$ , and the horizontal  $\mathbf{x}$  plane,  $v_{\perp}^{\alpha} = v_n(\hat{\mathbf{N}} \cdot \hat{\mathbf{x}}^{\alpha})$ , where  $\alpha = 1, 2$  labels the basis vectors in the  $\mathbf{x}$ - $\mathbf{y}$  plane [7]. Using the definitions (2) to (6) this yields the equations of motion,

$$\begin{aligned} \partial_t h = & \frac{\ell}{\tau} [\epsilon_+ (\lambda_1 + \lambda_2 \nabla^2 h + \lambda_3 \rho + \lambda_4 \rho \nabla^2 h) \\ & - \epsilon_- (\mu_1 \rho + \mu_2 \rho \nabla^2 h)] \\ & - \Gamma [-\sigma \nabla^2 h + \kappa_c \nabla^4 h - \kappa_c c_0 \nabla^2 \rho] + v_h + f_h \end{aligned} \quad (7)$$

for the height field and

$$\frac{\partial \rho}{\partial t} = -\nabla \cdot (\rho \mathbf{v}_{\perp}) + \nabla \cdot \left( D \nabla \frac{\delta F_{el}}{\delta \rho} \right) + j_+ - j_- + \nabla \cdot \mathbf{f}_{\rho}, \quad (8)$$

for the density field [8]. In Eq. (7),  $v_h = -\int \frac{d^2 q}{(2\pi)^2} e^{i\mathbf{q} \cdot \mathbf{x}} \frac{1}{4\eta|q|} \frac{\delta F_{el}}{\delta h_q(t)}$ , is the vertical component of the viscous flow ( $\eta$  is the solvent viscosity) induced at the membrane surface by the membrane elastic stresses [7]. We have ignored other sources of dissipation coming from intramembrane viscosity and bilayer friction [9]. The equations of motion also contain thermal noise sources having zero mean; in the Monge representation, the variance  $\langle |f_h(\mathbf{q}, t)|^2 \rangle = 2T \left[ \Gamma + (4\eta|q|)^{-1} \right]$ , while the variance of the vector noise  $\mathbf{f}_{\rho}$  is  $2TD$ . Note the source and sink terms  $j_{\pm}$  in Eq. (8) do not conserve particle material.

Let us first check if Eqs. (7,8) admit steady state solutions when we replace the noise terms by their means. We shall drop the hydrodynamic force for simplicity. Our subsequent analysis will be for a tensionless ( $\sigma = 0$ ) membrane with no spontaneous curvature ( $c_0 = 0$ ). We find *spatially homogeneous* steady states for which  $j_+ = j_-$ , which implies that in the steady state the density attains a uniform value given by

$$\rho_{\infty} = -\frac{e_+ \lambda_1}{e_+ \lambda_3 - e_- \mu_1}, \quad (9)$$

while the steady state height is a constant (which we take to be 0). Since  $\lambda_1 > 0$ , the above steady state holds when  $B \equiv e_+ \lambda_3 - e_- \mu_1 < 0$ . Is this steady state linearly stable to perturbations in  $h$  and  $\rho = \rho_{\infty} + \phi$ ? In momentum space, the linearised perturbations are given by,

$$\frac{d}{dt} \begin{pmatrix} h_q \\ \phi_q \end{pmatrix} = \begin{pmatrix} -\frac{\ell}{\tau} A q^2 - \kappa_c \Gamma q^4 & \frac{\ell}{\tau} B \\ -\frac{\ell^2}{a\tau} A q^2 & \frac{\ell^2}{a\tau} B - D\chi q^2 \end{pmatrix} \begin{pmatrix} h_q \\ \phi_q \end{pmatrix} \quad (10)$$

where  $A = e_+ \lambda_2 + \rho_\infty (e_+ \lambda_4 - e_- \mu_2)$ . The eigenvalues of the dynamical matrix for small  $q$  are

$$\lambda_{1,2} = \begin{cases} \frac{\ell^2}{a\tau} B - q^2 [D\chi + \frac{\ell}{\tau} A] \\ -q^4 [\kappa_c \Gamma - \frac{\ell}{(\ell^2/a\tau)} A D\chi/B] \end{cases} \quad (11)$$

The nonconservative  $\phi$  ensures that one of the modes is always ‘fast’ *i.e.*, has a nonzero relaxation rate at sufficiently long wavelength. If  $\ell A/\tau > -\min[D\chi, \kappa_c \Gamma (\ell^2/a\tau) |B|/D\chi] = -A^*$ , then both modes decay and the homogeneous flat steady state is stable. We calculate the equal-time height fluctuations about this steady state, by first restoring the thermal and non-thermal noises  $\epsilon_\pm = e_\pm + \delta\epsilon_\pm$ , in Eq. (10), fourier transforming with respect to  $\mathbf{x}$  and  $t$ , and then integrating the correlator with respect to frequency  $\omega$  to obtain,

$$\langle h_q(t) h_{-q}(t) \rangle = \frac{E}{q^2} + \frac{T}{\frac{\ell A}{\Gamma} q^2 + \kappa_c q^4} \quad (12)$$

for small  $q$ . The first term is a *purely nonequilibrium* contribution to the height fluctuations with a  $q^2$  dispersion and an amplitude  $E$  related to the variance of  $\delta\epsilon_\pm$  and the activity. The second term is a modification of the usual thermal correlator — the fission/fusion activity *suppresses* height fluctuations at small  $q$  through an activity-induced tension (see [5]) proportional to  $A$ . On the other hand, density correlations are short ranged with a correlation length  $\xi = B^{-1/2}$ .

If  $A < -A^*$ , then either one or both modes are unstable. The unstable massless mode grows as  $q^4$  for small  $q$ . Physically this instability is a consequence of the curvature dependent rate of fusion: an initial outward bump ( $\nabla^2 h < 0$ ) will promote a faster rate of fusion, adding on more  $h$ .

Going beyond linear stability analysis in the case  $A < -A^*$  requires a numerical simulation of Eqs. (7,8). It is convenient to work in dimensionless variables, where  $x \rightarrow x/\sqrt{\kappa_c/\chi}$ ,  $t \rightarrow t/(\kappa_c/D\chi)$ ,  $h \rightarrow h/\ell$  and  $\rho \rightarrow \rho/(\ell/a^2)$ . Using an Euler discretisation on a square grid of size  $N^2 = 100^2$ , we convert the differential equations to a coupled map. The spatial and temporal increments have been chosen to satisfy  $\Delta t < \Gamma^{-1} (\Delta x)^4$  and  $\Delta t < (\Delta x)^2$  to ensure numerical stability. For most of our analysis we have fixed  $\Delta x = 0.1$  and  $\Delta t = 10^{-4}$ . We have taken open boundary conditions and have used a large enough system to ensure that no finite size effects corrupt our interpretation. We report numerical results only for the linearly unstable case.

We start with the homogeneous steady state,  $h(\mathbf{x}, 0) = 0$  and  $\rho = \rho_\infty$ , and set the non-thermal noises to their average values,  $\epsilon_\pm = e_\pm$ . Introduce a small bump, a paraboloid of height  $L_0$  and width  $w_0$  smoothly connected to the rest of the membrane. The peak height

$L(t)$  and the width  $w(t)$  grow initially, the width then saturates at  $q_*^{-1} \sim |A|^{-1/2}$ , the length scale corresponding to the fastest growing mode determined from the linear analysis. The height now grows exponentially as  $L(t) \sim \exp(A^2 t)$  (Fig. 2). Beyond this linear regime, whose time scale is set by  $A$ , the nonlinear term  $\nu \rho \nabla^2 h$  (where  $\nu \equiv e_+ \lambda_4 - e_- \mu_2$ ) starts becoming comparable. The sign of  $\nu$  dictates the subsequent evolution [10]. If  $\nu < 0$ , the nonlinear term *accelerates* the growth, producing a long thin tubule (Fig. 2). Since the local curvature of the membrane becomes positive in the region where the main peak joins the rest of the membrane, this gives rise to side branches which dig into the membrane at a much slower rate (Fig. 2). The resulting morphology is a long tubule which grows very fast. This fast growth may eventually be halted by molecular processes not contained in our coarse-grained model, leading to a fissioning of the tubule from the parent membrane.

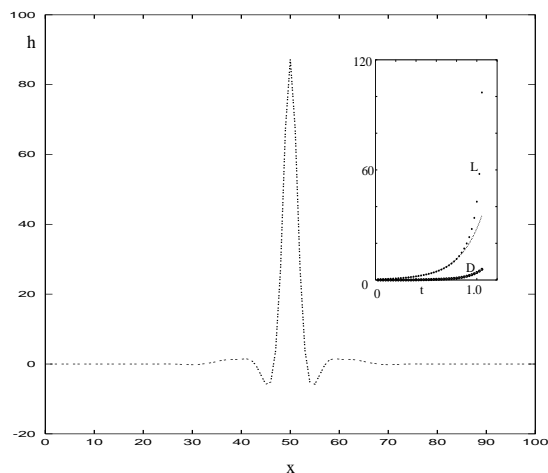


FIG. 2. Tubule configuration (obtained by rotating the profile about the vertical axis) at  $t = 1.1$  when  $\nu < 0$ . Inset shows the peak height  $L$  and the depth of the side branch  $D$  (dashed line is the initial exponential growth of  $L$ ). The parameters  $\nu = -0.012$  and  $A = -0.16$ .

When  $\nu > 0$ , the exponential rise of the peak height is cut off by a *decrease* in the rate  $j \equiv j_+ - j_-$ . At the same time the density at the peak diffuses out into the flanks in such a way as to compensate for the increase coming from the addition of ‘particles’. This leads to a saturation of the density at the peak and asymptotically approaches  $\rho_s = -e_+ \lambda_2/\nu$ . The depth of the flanks increases exponentially fast till it is comparable with the slowly increasing peak height  $L$ . The resulting structure is a folded configuration as in Fig. 3.

So far we had set the non-thermal noises  $\epsilon_\pm$  to their average values; we had therefore needed an initial bump on the membrane to seed the growth of tubules. The situation is unchanged if instead we let  $\epsilon_\pm(\mathbf{x}, t) = e_\pm + \delta\epsilon_\pm(\mathbf{x}, t)$ , where the fluctuations are uncorrelated

in space and time. In practice, this initial localised perturbation about the steady state may be achieved by either phase separation of different lipid species constituting the membrane [2] or noise. If we however set  $\epsilon_{\pm}(\mathbf{x}, t) = \epsilon_{\pm}(t)\delta(\mathbf{x})$ , where  $\epsilon_{\pm}(t)$  is stochastic, then the membrane *spontaneously creates a bump at the fusion site*, growing exponentially fast.

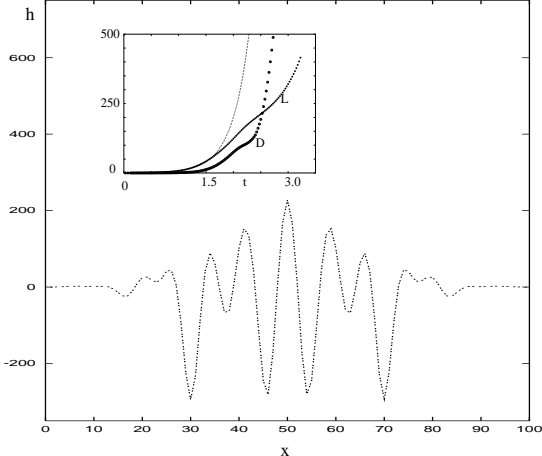


FIG. 3. Folded configuration (obtained on rotation about the vertical) at  $t = 2.6$  when  $\nu > 0$ . Inset shows the height of the central peak  $L$  and the largest depth of the folds  $D$  (dashed line is the initial exponential growth of  $L$ ). The parameters  $\nu = 0.012$  and  $A = -0.14$ .

The tubular extensions produced when  $\nu < 0$  look similar to the structures exhibited by the sorting endosome associated with the endocytic pathway of transferrin and LDL proteins. The sorting endosome is seen to possess several tubular structures of width  $\approx 50\text{nm}$  which grow to a length of about a micron before peeling off from the parent structure [2]. On the other hand, the folded structures produced when  $\nu > 0$  are most dramatically exhibited in a closed membrane, which may be studied using a dynamical triangulation monte carlo modified to add and subtract particles [11].

Such tubulation or folded morphologies could also be generated if the ‘particles’ depositing on and ‘evaporating’ from the membrane are isolated proteins. The rates of these events may be altered by the action of some drug, such as Brefeldin-A. Our analysis suggests that such deposition-evaporation of proteins from a membrane could result in tubulation [12].

A second look at Eqs. (7,8) allows us to make some definite predictions. We see that the surface tension, which is the coefficient of the  $\nabla^2 h$  term, gets renormalized by an ‘activity induced’ factor,  $\tilde{\sigma} = \sigma + \ell A/\Gamma$ . This renormalization is also reflected in the form of the correlators, Eq. (12). Alternatively, *applying a tension  $\sigma$  to the membrane will affect the rate of fusion/fission events* [13].

The activity induced tension is in general inhomogeneous since the ‘activity’  $A$  may be space dependent. This gives rise to gradients in the activity induced surface tension, driving flow of membrane constituents to-

wards regions of lower tension. Ignoring bilayer friction, the velocity of this Marangoni flow may be written as  $\mathbf{v}_{\perp} = -\frac{\xi^2}{\mu}\nabla\tilde{\sigma}$ , where  $\mu$  is the in-plane shear viscosity and  $\xi$  is a length scale associated with the ‘particle’ size. The direction of flow is such that the membrane constituents will move towards the tubular extensions produced as a result of the activity.

In future we would like to study the effects of stochastic fusion/fission of ‘particles’ on a closed fluid membrane [11], and to explore the complete nonequilibrium steady state diagram by solving the stochastic equations (7,8).

We thank P. B. S. Kumar and especially S. Mayor and S. Ramaswamy for several illuminating discussions and critical readings of the manuscript. We thank J. Prost for informing us of a short note on the same subject [14]. MR thanks the Department of Science and Technology, India for a Swarnajayanti Fellowship.

\* email : madan@rri.ernet.in

† email : sarasij@rri.ernet.in

- [1] B. Alberts *et. al.*, in *Molecular Biology of the Cell*, 3<sup>rd</sup> Ed. (Garland Publ., NY, 1994).
- [2] S. Mukherjee and F. Maxfield, *Traffic* **1**, 203 (2000).
- [3] J. C. Hay and R. H. Scheller, *Curr. Opin. Cell Biol.* **9**, 505 (1997) and other articles in this issue.
- [4] P. Canham, *J. Theor. Biol.* **26**, 61 (1970); W. Helfrich, *Z. Naturforsch.* **28C**, 693 (1973).
- [5] S. Ramaswamy, J. Toner and J. Prost, *Phys. Rev. Lett.* **84**, 3494 (2000).
- [6] We should distinguish this active fusion/fission process from the deposition/evaporation of particles onto/from an interface separating two bulk coexisting phases.
- [7] W. Cai and T. C. Lubensky, *Phys. Rev. Lett.* **73**, 1186 (1994).
- [8] In principle, the equations of motion in the case when the ‘particles’ are isolated proteins should include the height  $h$ , the nonconserved protein density  $\rho$  and the conserved lipid density  $c$ . The lipid density however does not couple to the other two fields.
- [9] U. Seifert, *Adv. Phys.* **46**, 13 (1997).
- [10] There are higher order nonlinear terms of the KPZ type which will saturate the growth at later times. However in biological cells, other processes not included in our analysis will have intervened by this time leading to a pinch-off of the tubule.
- [11] P. B. S. Kumar, Sarasij R. C. and M. Rao, in preparation.
- [12] We thank S. Mayor for a detailed discussion.
- [13] M. P. Sheetz and J. Dai, *Trends Cell Biol.* **6**, 85 (1996).
- [14] J. Prost, *Biol. Skr. Dan. Vid. Selsk.* **49**, 193 (1998).